Space Vector Based Hybrid PWM Algorithm for Direct Torque Controlled Induction Motor Drives for Reduced Common Mode Voltage

V. Anantha Lakshmi[1] V. C. Veera Reddy[2]
[1]E.E.E Department, G. Pulla Reddy Engineering College, Kurnool, Andhra Pradesh, India, v.al@rediffmail.com
[2]E.E.E Department, S.V. University, Tirupathi, Andhra Pradesh, India, veerareddyj1@rediffmail.com

M. Surya Kalavathi[3]
[3]E.E.E Department, J.N.T. University, Kukatpally, Hyderabad, Andhra Pradesh, India,
munagala12@yahoo.co.in

Abstract: *Direct torque control (DTC) is gaining importance in the industry due to its simplicity and dynamic performance. In spite of its simplicity it generates high level common mode voltage (CMV) variations and steady state ripples. This paper presents a simplified space vector based hybrid pulse width modulation (HPWM) technique for the reduction of CMV and steady state ripple in direct torque controlled induction motor drives. In the proposed approach different active zero state PWM (AZPWM) sequences are considered in which two active voltage vectors are utilized with two active and opposite voltage vectors for composition of reference voltage vector and a procedure is presented for designing a new HPWM technique involving four AZPWM sequences for reduced current ripple. To validate the proposed PWM algorithm, numerical simulation studies have been carried out using MATLAB-Simulink and results are presented and compared.*

Key words*: direct torque control, induction motor drives, active zero state PWM, HPWM*

1. Introduction

Dynamic performance of PWM inverter fed ac motor drives has been improved with the advent of fast switching semi conductor devices like IGBT, there by increasing the switching frequency of inverter. The high $\frac{dv}{dt}$ produced by PWM inverters caused several unexpected problems such as shaft voltages, bearing currents and breakdown insulation [1]. Many studies for reducing the CMV have been progressed. These studies however focused on the design of common mode choke, 4-phase inverter and various types of active filters [2-4]. Since these methods require additional hardware and has drawbacks of increase in inverter weight and volume which are unavoidable. Direct Torque Control (DTC) is an emerging technique for controlling the PWM inverter-fed induction motor drives when compared with vector controlled induction motor. In spite of its simplicity, DTC has certain draw backs such as high steady state ripples in torque, flux and current which leads to incorrect speed estimation and generation of high level CMV variations [5-7]. To reduce steady state ripple and to get constant switching frequency operation, a space vector PWM technique has been proposed. In this approach, two active voltage vectors and two zero voltage vectors are utilized to match the reference volt–seconds. This technique also generates high level CMV variations due to the presence of zero voltage vectors [8-9]. Different AZPWM algorithms are proposed for the reduction of CMV in which instead of using zero voltage vectors, active voltage vectors are utilized for composing the reference voltage vector [10]. These methods reduce CMV variations but they still suffer from steady state ripples. A substantial reduction in torque, flux and current ripple can be obtained using HPWM method in which the expressions for mean square stator flux ripple over a sub cycle are derived for different sequences [11-12]. This technique also suffers from CMV variations due to presence of zero voltage vectors. So in this paper in order to reduce the steady state ripple and CMV variations space vector based HPWM technique is developed for induction motor drives and applied to DTC. In the proposed approach, different AZPWM sequences are considered. Though these methods restrict CMV to $+V_{dc}/6$ or $-V_{dc}/6$ but still suffer from steady state ripples. In order to reduce these ripples, a HPWM algorithm is developed in which flux ripple analysis for each AZPWM sequence is done and then comparing each AZPWM sequence with respect to other sequence at various modulation indices the sequence with minimum flux ripple is obtained. As all the sectors are symmetric in this paper first sector is considered. HPWM based DTC has less total harmonic distortion (THD) and CMV variations when compared with CDTC.

2. MODELING OF INDUCTION MOTOR

The dynamic model of a 3-ϕ induction motor in stationary reference frame is given by

$$\begin{bmatrix} V_{qs} \\ V_{ds} \\ V_{qr} \\ V_{dr} \end{bmatrix} = \begin{bmatrix} R_S + L_S P & 0 & L_m P & 0 \\ 0 & R_S + L_S P & 0 & L_m P \\ L_m P & -L_m w_r & R_r + L_r P & -L_r w_r \\ L_m w_r & L_m P & L_r w_r & R_r + L_r P \end{bmatrix} \begin{bmatrix} i_{qs} \\ i_{ds} \\ i_{qr} \\ i_{dr} \end{bmatrix} \quad (1)$$

Where $\omega_r = d\theta/dt$ and $p = d/dt$
The stator and rotor flux linkages in the stator reference frame are defined as

$$\lambda_{qs} = L_s i_{qs} + L_m i_{qr}$$
$$\lambda_{ds} = L_s i_{ds} + L_m i_{dr}$$
$$\lambda_{qr} = L_r i_{qr} + L_m i_{qs} \quad (2)$$
$$\lambda_{dr} = L_r i_{dr} + L_m i_{ds}$$

The instantaneous electromagnetic torque of a 3-phase induction machine in stationary reference frame is given by $T_e = \frac{3}{2}\frac{P}{2}\left(\lambda_{ds} i_{qs} - \lambda_{qs} i_{ds}\right)$ (3)

Where P is the number of poles.

3. Conventional DTC

The block diagram of conventional DTC is shown in Fig.1. Actual values of torque and flux are obtained from adaptive motor model. These actual values of torque and flux are compared with reference values of torque and flux using torque and flux comparators. A Three level torque and two level flux hysteresis controllers are used according to the outputs of the torque controller and the sector estimation of λ_s, appropriate voltage vectors are selected from the optimal switching table. This switching table selects the suitable voltage vector to limit torque and flux errors with in the hysteresis band, which results in direct control. Though DTC has quick torque response it suffers from high steady state ripples in torque, flux and current and high CMV variations.

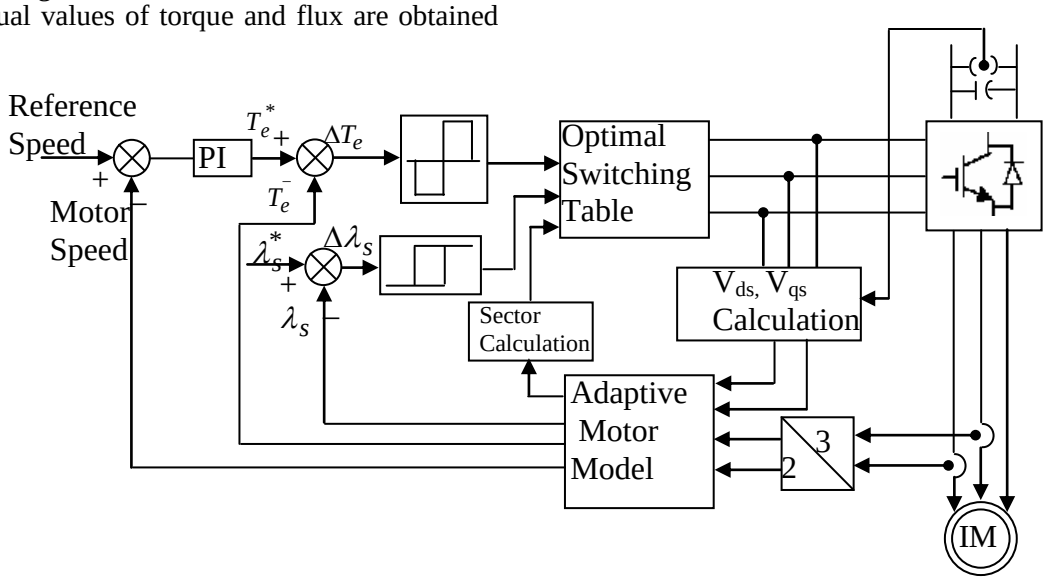

Fig-1: Block diagram of Conventional DTC

4. Proposed DTC

Table – I: CMV variations for different Inverter Switching States:

State	V_{ao}	V_{bo}	V_{co}	V_{com}
V_0	$-V_{dc}/2$	$-V_{dc}/2$	$-V_{dc}/2$	$-V_{dc}/2$
V_1	$V_{dc}/2$	$-V_{dc}/2$	$-V_{dc}/2$	$-V_{dc}/6$
V_2	$V_{dc}/2$	$V_{dc}/2$	$-V_{dc}/2$	$V_{dc}/6$
V_3	$-V_{dc}/2$	$V_{dc}/2$	$-V_{dc}/2$	$-V_{dc}/6$
V_4	$-V_{dc}/2$	$V_{dc}/2$	$V_{dc}/2$	$V_{dc}/6$
V_5	$-V_{dc}/2$	$-V_{dc}/2$	$V_{dc}/2$	$-V_{dc}/6$
V_6	$V_{dc}/2$	$-V_{dc}/2$	$V_{dc}/2$	$V_{dc}/6$
V_7	$V_{dc}/2$	$V_{dc}/2$	$V_{dc}/2$	$V_{dc}/2$

a. Common Mode Voltage (CMV)

According to the switching states of a 3-ϕ, voltage source inverter, the CMV can be expressed as

$$V_{com} = \frac{\left(V_{ao} + V_{bo} + V_{co}\right)}{3} \quad (4)$$

Where V_{ao}, V_{bo} and V_{co} are the inverter pole voltages.

CMV is different from zero, when the drive is fed from an inverter. It can be shown that DC-link voltage and switching pattern of the inverter decides the CMV, regardless of the ac machine impedance. There are eight output voltage vectors in which six are active voltage vectors and remaining two vectors are zero voltage vectors with totally eight possible switching states of the inverter. Table-I indicates the CMV for different switching states. From the table it can be

observed that CMV is very high for zero voltage vectors. In order to reduce CMV usage of zero voltage vectors are avoided in the proposed methods.

b. AZPWM Algorithms

Different switching patterns for each sector of the AZPWM techniques are shown in Table-II. From the table, it can be observed that in sector-I of AZPWM1 method two active voltage vectors (V_1, V_2) are used with two opposite voltage vectors (V_3, V_6) . Any one of the three pairs V_1-V_4, V_2-V_5, V_3-V_6 can be used. All the four AZPWM methods have CMV of $+V_{dc}/6$ or $-V_{dc}/6$.

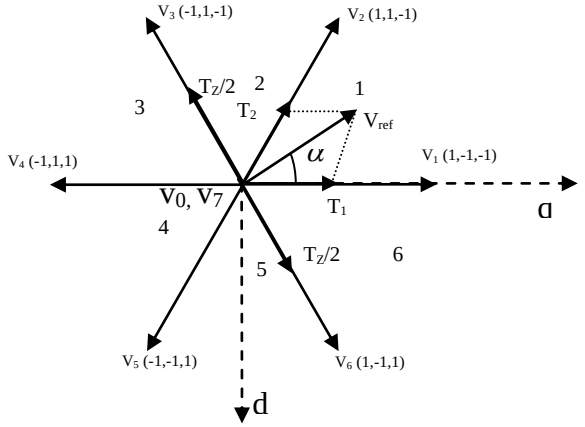

Fig.2 Construction of reference voltage vector in sector -I of AZPWM1 sequence

In the AZPWM method, the reference voltage space vector (V_{ref}) or sample is obtained by substituting the various sampled voltage vectors at each time interval, T_s, referred to as sub cycle in the average sense. Suppose consider AZPWM1 sequence and assume that sample lies in first sector, V_{ref} at α angle can be generated by using two active opposite voltage vectorsV_3 and V_6 in combination with two adjacent active voltage vectors V_1 and V_2 for time durations T_1, T_2 and T_z respectively within the sampling time period T_s. Construction of reference voltage vector is shown in Fig 2.

$$T_1 = M * \frac{3}{\pi} * \frac{Sin(60^o - \alpha)}{Sin(60^o)} * T_s \quad (5)$$

$$T_2 = M * \frac{3}{\pi} * \frac{Sin\alpha}{Sin60^o} * T_s \quad (6)$$

Where M is the modulation index and given by $M = \frac{\pi * V_{ref}}{2 * V_{dc}}$.

To keep the switching frequency constant, the remainder of the time is spent on the two active opposite voltage vectors states, that is

$$T_z = T_s - (T_1 + T_2) \quad (7)$$

The zero state time is divided equally among the two voltage vectors V_3 and V_6. The voltage vector V_6 is applied at the end of sampling time whereas, the voltage vector V_3 is applied at the beginning of the sampling time in sector-I. Both the voltage vectors are applied for same duration. Though AZPWM methods reduce CMV they still suffer from high steady state ripples. While comparing the ripple characteristics of different AZPWM methods, number of commutations (N_c) per sub cycle must be considered. Except AZPWM4 all methods have the same N_c. In order to obtain the same N_c in each method, the switching frequency of each method must be divide by K_f factor.

Table -II: Switching sequences of different AZPWM algorithms

PWM METHOD	S-I	S-II	S-III	S-IV	S-V	S-VI
AZPWM1	3216-6123	1234-4321	5432-2345	3456-6543	1654-561	5612-2165
AZPWM2	1124-4211	5322-2235	3346-6433	1544-4451	5562-2655	3166-6613
AZPWM3	2215-5122	6233-3326	4431-1344	2455-5542	6653-3566	4611-1164
AZPWM4	6213-3126	4231-1324	2435-5342	6453-3546	4651-1564	2615-5162

c. Expressions for root mean square(rms) flux Ripple

The difference between the applied voltage vector and the reference voltage vector is defined as the stator flux ripple vector. The instantaneous voltage ripple vectors in corresponding to the active vector 1, active vector 2 and active vectors acting as zero vectors for AZPWM1 method along with its corresponding d-axis and q-axis stator flux ripple components are shown in Fig.3.

All the AZPWM methods maintain volt-seconds balance to generate a voltage space vector, which equals to reference space vector in an average sense. The error volt-seconds corresponding to ripple voltage vectors can be developed as given in [14]. For the AZPWM1 sequence the d-axis stator flux ripple components are given in terms of D and P and q-axis stator flux ripple components are given in terms of Q_1,Q_2,Q_3 and Q_6 which are defined as (8)-(11).

$$V_{rip1}T_1 = \frac{2}{3}V_{dc}\sin\alpha T_1 + j(\frac{2}{3}V_{dc}\cos\alpha - V_{ref})T_1 = D + jQ_1 \quad (8)$$

$$V_{rip2}T_2 = \frac{2}{3}V_{dc}\sin(60^0-\alpha)T_2 + j(\frac{2}{3}V_{dc}\cos(60^0-\alpha) - V_{ref})T_2 \quad = -D + jQ_2 \qquad (9)$$

$$V_{rip3}T_{\frac{Z}{2}} = -\frac{2}{3}V_{dc}\sin(60^0+\alpha)T_{\frac{Z}{2}} - j(\frac{2}{3}V_{dc}\cos(60^0+\alpha) + V_{ref})T_{\frac{Z}{2}} = -P - jQ_3 \qquad (10)$$

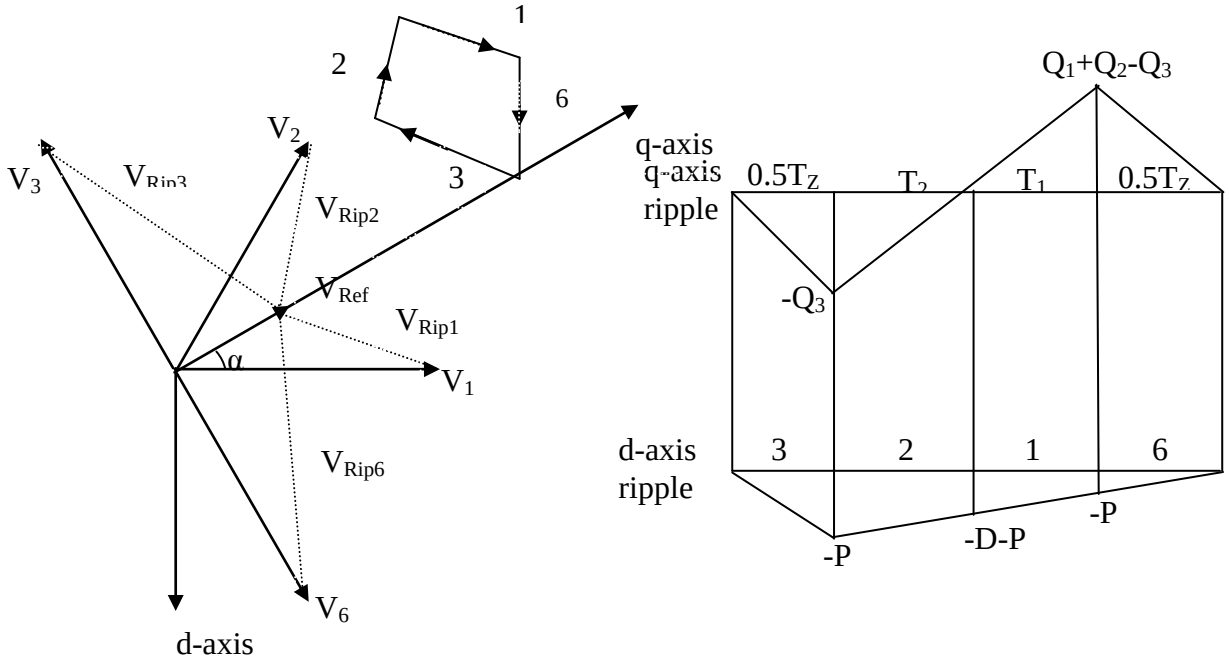

Fig.3 Variations of stator flux ripple vector over a sampling period and its corresponding d- axis and q-axis components of AZPWM1 sequence

$$V_{rip6}T_{\frac{Z}{2}} = \frac{2}{3}V_{dc}\sin(60^0+\alpha)T_{\frac{Z}{2}} + j(-\frac{2}{3}V_{dc}\cos(60^0+\alpha) + V_{ref})T_{\frac{Z}{2}} = P + jQ_6 \qquad (11)$$

Over a sampling interval, the mean square stator flux ripple can be calculated as

$$F_{rms}^2 = \frac{1}{T_s}\int_0^{Ts} F_{q,rip}^2 dt + \frac{1}{T_s}\int_0^{Ts} F_{d,rip}^2 dt \qquad (12)$$

From Fig .3 the expression for mean square ripple over a sub cycle for AZPWM1 sequence can be obtained as given in (13) using the values of d-axis and q-axis ripple at the switching instants. Similarly, expression for mean square ripple for other sequences can be derived in the same manner.

$$F_{3216}^2 = \frac{1}{3}(0.5Q_3)^2.\frac{T_z}{T_s} + \frac{1}{3}\left(Q_3^2\right)\frac{T_2}{T_s} + \frac{1}{3}.(Q_1+Q_2-Q_3)^2.\frac{T_1}{Ts} + (Q_1+Q_{2-}Q_3)^2\frac{0.5T_z}{T_s} + (Q_1+Q_{2-}Q_3)^2\frac{0.5T_z}{T_s}$$
$$+\frac{1}{3}\left(0.5P^2\right)\frac{Tz}{T_s} + \frac{1}{3}\left(0.5P^2\right)\frac{T_z}{T_s} + \frac{1}{3}\left(3P^2+D^2+3PD\right)\frac{T_2}{T_s} + \frac{1}{3}\left(D^2+3P^2+3PD\right)\frac{T_1}{T_s} \qquad (13)$$

d. Hybrid PWM

To reduce the complexity involved in CDTC, different AZPWM sequences are considered in the proposed approach. Although the four AZPWM methods reduce CMV variations but still they suffer from steady state ripples. To reduce these ripples a new Hybrid PWM algorithm is is proposed. In the proposed approach, flux ripple analysis of each AZPWM sequence is derived in terms of α , V_{ref}, V_{dc} and switching times.

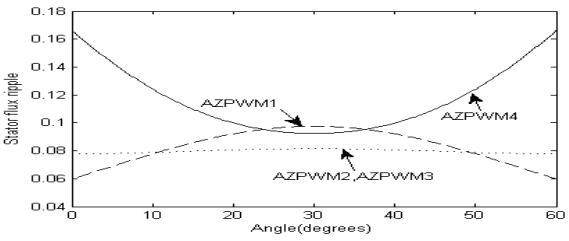

(a) M=0.55

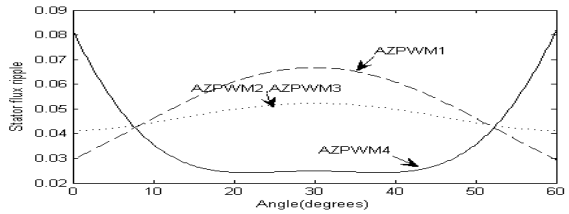

(b) M=0.72

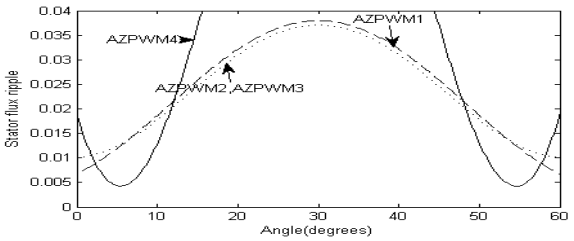

(c) M=0.9

Fig. 4 Variations of RMS stator flux ripple for different modulation indices

As AZPWM2, AZPWM3 exhibit same ripple characteristics only AZPWM3 is considered in this paper. Then by comparing AZPWM1, AZPWM3, AZPWM4 sequences with respect to each other sequences at various modulation indices the sequence with minimum flux ripple is obtained. This sequence is then fed to DTC based induction motor drive. As all the sectors are symmetric, rms stator flux ripple characteristics for a period of 60^0 for different switching sequences are plotted at different modulation indices (M) and are given in Fig 4.From Fig 4(a) - 4(c), it can be observed that the AZPWM3 algorithm gives superior performance at lower modulation indices (M=0.55) when compared with other sequences, AZPWM4 gives superior performance at M=0.72 and at M=0.9 AZPWM2 gives superior performance when compared with other sequences (near the edges AZPWM4 is better). Hence a hybrid PWM technique is developed which results in less ripple current.

e. Proposed hybrid PWM based DTC

The block diagram of proposed PWM algorithms based DTC is shown in Fig.5. In this method, actual values of d-axis and q-axis fluxes are obtained from the adaptive motor model. These actual values of fluxes are compared with reference values and an error in flux is obtained which when divided by the sampling time period gives a reference voltage vector used for direct control of torque and flux. These d-axis and q-axis reference voltage vectors are then fed to the PWM block. Then by using above PWM algorithm procedure, the actual gating pulses can be generated which are then fed to the inverter.

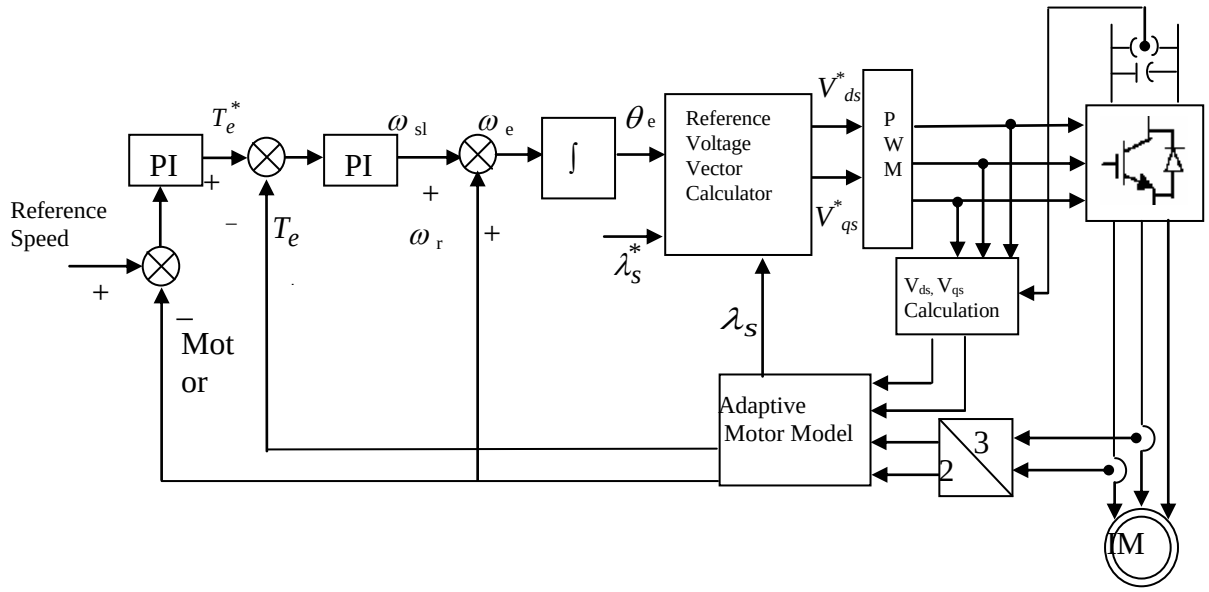

Fig. 5 Block diagram of proposed hybrid PWM based DTC algorithm

5. Simulation Results and Discussion

To validate the proposed PWM algorithm, numerical simulation studies have been carried out by using *Matlab* /Simulink. For the simulation, the reference flux is taken as 1wb and starting torque is limited to 45 N-m. For the simulation studies, a 3-phase, 400V, 4 kW, 4-pole, 50 Hz, 1470 rpm induction motor has considered. The parameters of the given induction motor are as follows: R_s=1.57ohm, R_r=1.21ohm, L_m= 0.165H, L_s= 0.17H, L_r= 0.17 H and J= 0.089 Kg - m^2. The simulation results are shown in Fig.6-Fig.20 for CDTC based induction motor drive and AZPWM based DTC for various conditions such as steady state, CMV variations and THD of stator current. From the simulation results, it can be observed that CDTC and AZPWM based DTC has high steady state ripples in flux, torque and current. So, in order to reduce the

steady state ripples hybrid PWM based DTC is developed in the proposed approach. Simulation results for the proposed hybrid PWM based DTC are given in Fig.21-Fig.23. From the simulation results, it can be observed that the proposed hybrid PWM method reduce the steady state flux, torque and current ripples of direct torque controlled induction motor drive when compared with AZPWM methods. As CDTC operates at variable switching frequency, switching frequency is considered at 5KHZ. The drawback of CDTC is variable switching frequency and high ripples in torque, flux and current ripples. So in order to overcome the draw backs of CDTC, AZPWM methods are considered for maintaining constant switching frequency operation.

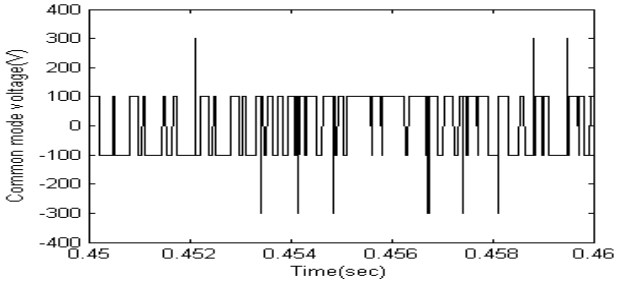

Fig 6 CMV variations in CDTC

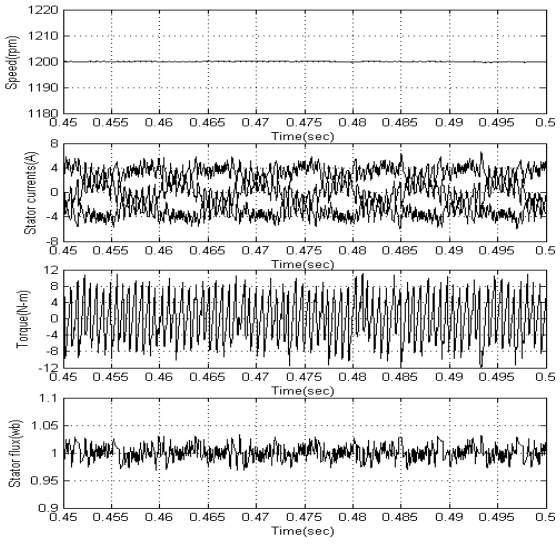

Fig 7 Steady state plots in CDTC algorithm

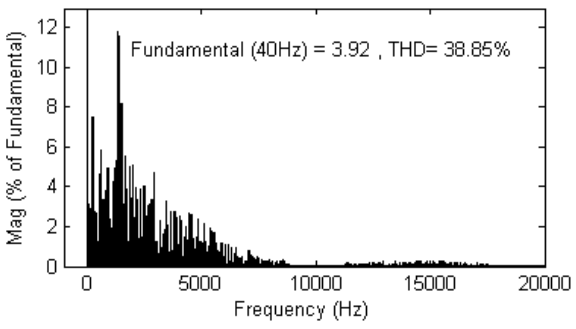

Fig 8 THD of stator current in CDTC algorithm

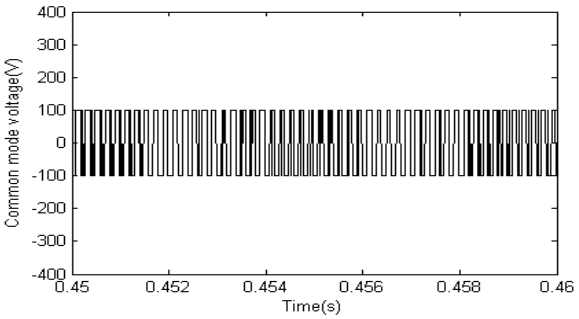

Fig 9 CMV variations in AZPWM1 based DTC algorithm

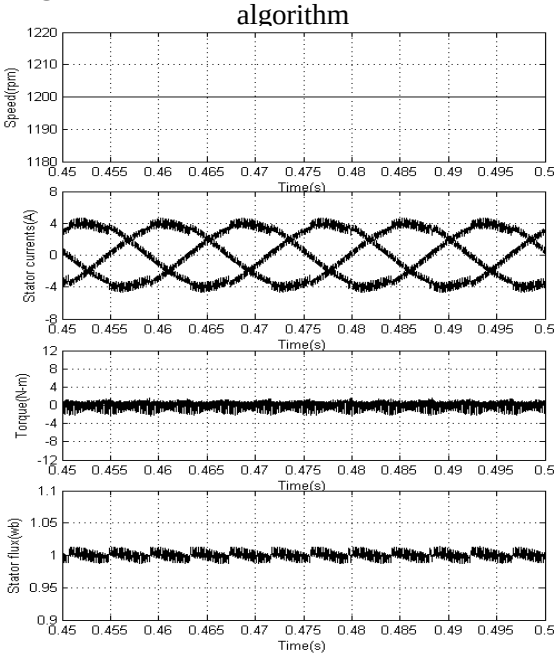

Fig 10 Steady state plots in AZPWM1 based DTC algorithm

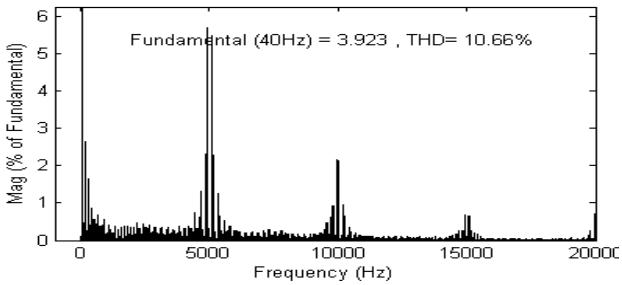

Fig 11 THD of stator current in AZPWM1 based DTC algorithm

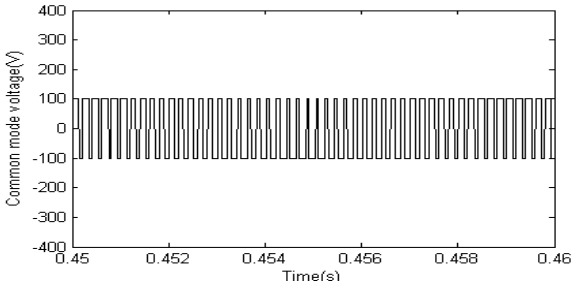

Fig 12 CMV variations in AZPWM2 based DTC algorithm

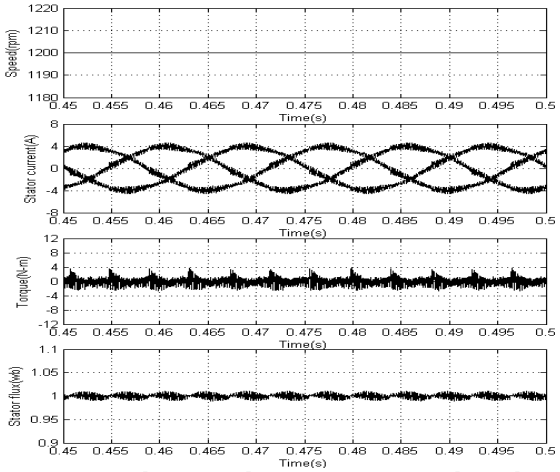

Fig 13 Steady state plots in AZPWM2 based DTC algorithm

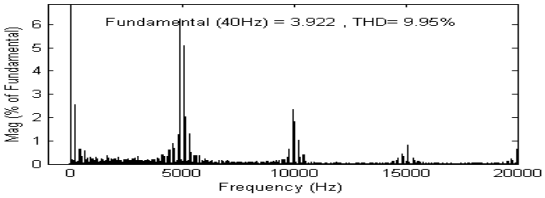

Fig 14 THD of stator current in AZPWM2 based DTC algorithm

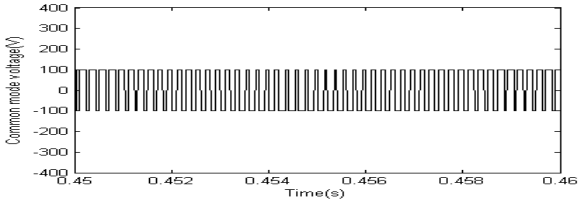

Fig 15 CMV variations in AZPWM3 based DTC algorithm

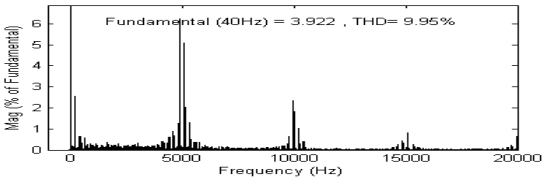

Fig 16 THD of stator current in AZPWM3 based DTC algorithm

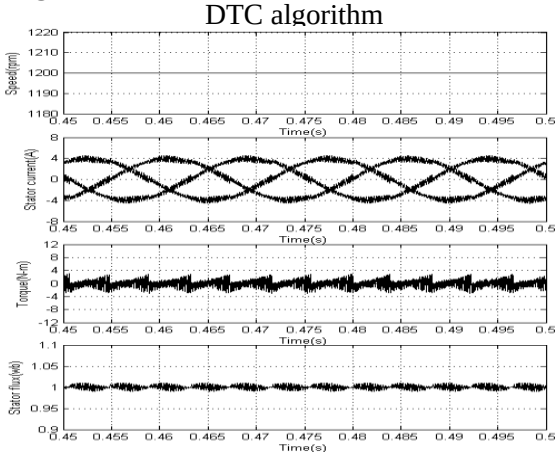

Fig 17 Steady state plots in AZPWM3 based DTC algorithm

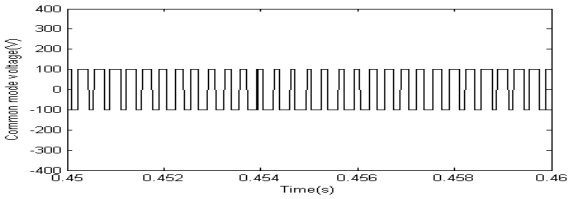

Fig 18 CMV variations in AZPWM4 based DTC algorithm

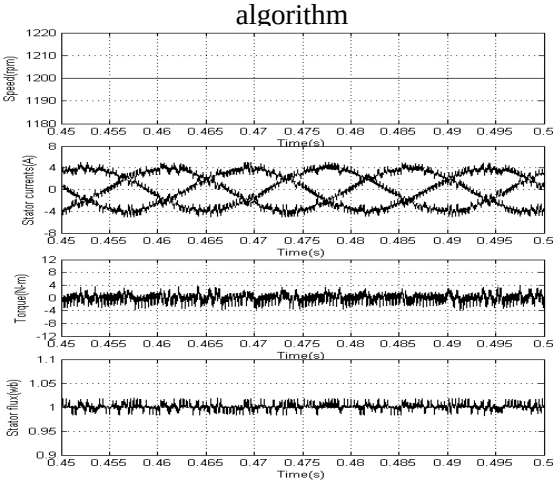

Fig 19 Steady state plots in AZPWM4 based DTC algorithm

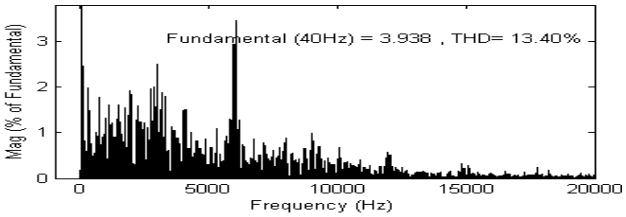

Fig 20 THD of stator current in AZPWM4 based DTC algorithm

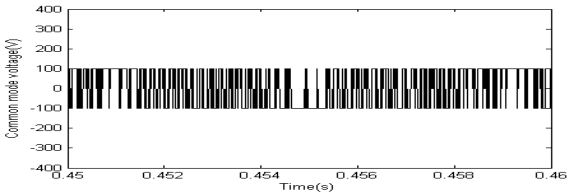

Fig 21 CMV variations in hybrid PWM based DTC algorithm

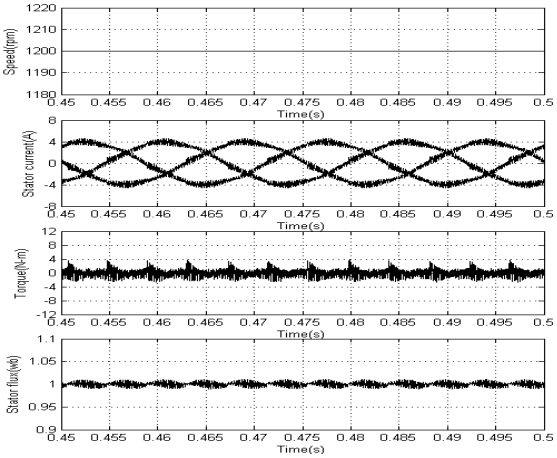

Fig 22 Steady state plots in hybrid PWM based DTC algorithm

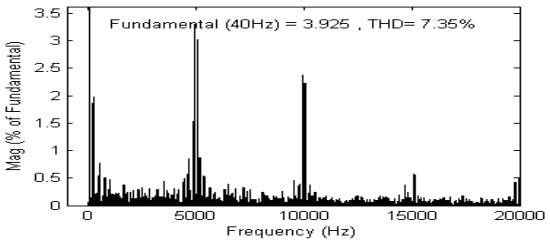

Fig 23 THD of stator current in hybrid PWM based DTC algorithm

6. Conclusions

Though DTC is simple, it generates high CMV variations with the usage of zero voltage vectors. Moreover steady state ripples in current, torque and flux are also high for CDTC. To over come these problems, in this paper different AZPWM algorithms are developed in which active voltage vectors are used for the composition of reference voltage vector in each sector, so that CMV changes from $+V_{dc}/6$ or $-V_{dc}/6$ instead of $+V_{dc}/2$ or $-V_{dc}/2$ as in CDTC.

Though the proposed AZPWM methods reduce the CMV but still have high stator flux, torque and current ripples in steady state. So, in order to reduce these steady state ripples HPWM algorithm is developed based on the flux ripple analysis of different AZPWM sequences and proposed for DTC. From the simulation results, it can be observed that the HPWM has less THD of stator current when compared with AZPWM methods and CDTC.

7. References

1.J.Erdman, R.J.Kerkman, D.W.Schlegel, and G. L. Skibinski,: "*Effect of PWM inverters on AC motor bearing currents and shaft voltages*", In: IEEE Trans. Ind. Applicat., vol. 32,Mar/Apr. 1996,pp,250-259.

2.M.M.Swamy, K.Yamada, and T.Kume,: "*Common mode current attenuation techniques for use with PWM drives*," In: *IEEE Trans. Power Electron.,* vol. 16, no.2,pp. 248-255,Mar. 2001.

3. Satoshi Ogasawara, Hirofumi Akagi ,: "*Suppression of Common-mode Voltage in a PWM Rectifier/Inverter System*",In: IEEE Trans, Ind. Applicat. ,vol. 3, pp. 2015-2021,Sep.-Oct 2001.

4.Yaxiu Sun, Abdolreza Esmaeli ,: Li Sun, Erliang Kang"*Investigation and Suppression of Conducted EMI and Shaft Voltage in Induction Motor Drive System*", In: IEEE Trans, on Int. Con. & Aut. , Jun 21-23, 2006

5. Domenico Casadei, Francesco Profumo, Giovanni Serra, and Angelo Tani,: "*FOC and DTC: Two Viable Schemes for Induction Motors Torque Control*", In: *IEEE Trans. Power Electron.,* vol. 17, no.5, Sep, 2002, pp. 779-787.

6. Isao Takahashi and Toshihiko Noguchi,: "*A new quick-response and high-efficiency control strategy of an induction motor*," In: *IEEE Trans.Ind. Applicat.*, vol. IA-22, no.5, Sep/Oct 1986, pp. 820-827.

7. Marcello Pucci, Gianpaolo Vitale and Giansalvo Cirrincione,: "*A new direct torque control strategy for the minimization of common-mode emissions*",In: *IEEE Trans. Ind. Appl.*,vol.4, no.2,Mar/Apr, 2006.

8. Thomas G. Habetler, Francesco Profumo Michele Pastorelli and Leon M. Tolbert ,: "*Direct Torque Control of Induction Machines Using Space Vector Modulation*", In: IEEE Trans. Ind. Appl., Vol. 28, No.5, pp. 1045-1053, Sep/Oct, 1992.

9. Heinz Willi Van Der Broeck, Hans-Christoph Skudelny, Member, IEEE, and Georg Viktor Stanke ,: *" Analysis and Realization of a Pulsewidth Modulator Based on Voltage Space Vectors*" In: IEEE Trans. Ind. Appl.,vol.24, no.1,Jan/Feb, 1998.

10. Ahmet M.Hava and Emre Un,: "*Performance Analysis of Reduced Common-Mode Voltage PWM Methods and Comparison With Standard PWM Methods for Three-Phase Voltage-Source Inverters*" In: IEEE Trans. Power Electron., vol. 24, no.1, Jan, 2009, pp. 241-252.

11. G.Narayanan, V. T. Ranganathan: "*Analytical Evaluation of Harmonic Distortion in PWM AC Drives Using the Notion of Stator Flux Ripple*" ,In: IEEE Trans on Power Electronics, vol. 20, No. 2, March 2005.

12. G.Narayanan, Di Zhao, H. Krishnamurthy and Rajapandian Ayyanar,: "*Space vector based hybrid techniques for reduced current ripple*",In: IEEE Trans.Ind. Applic., Vol. 55, No.4, pp.1614-1626, April 2008.